RESEARCH PAPER

Magnetic amine-functionalized graphene oxide as a novel and recyclable bifunctional nanocatalyst for solvent-free synthesis of pyrano[3,2-c]pyridine derivatives

Shahnaz Rostamizadeh [1,*], Asieh Hemmasi [1], Negar Zekri [2]

[1] Department of Chemistry, Faculty of Science, K.N.Toosi University of Technology, Tehran, Iran

[2] Faculty of Chemistry and Chemical Engineering, Malek-Ashtar University of Technology, Tehran, Iran

ARTICLE INFO

Article History:
Received 16 September 2016
Accepted 24 November 2016
Published 15 January 2017

Keywords:
Characterization
Fe_3O_4-GO-NH_2
Magnetically recoverable - nanocatalyst
Pyrano[3,2-c]pyridine derivatives
Solvent-free

ABSTRACT

The new magnetic amine-functionalized graphene oxide (Fe_3O_4-GO-NH_2) nanocatalyst was prepared through the reaction of 3-aminopropyltriethoxysilane (APTES) with magnetic graphene oxide (Fe_3O_4-GO). It was characterized by XRD, TEM, SEM, FT-IR and EDX techniques. The intrinsic carboxylic acids on the edges of Fe_3O_4-GO along with the amine groups post grafted to the surface of Fe_3O_4-GO led to preparation of an acid-base bifunctional magnetically recyclable nanocatalyst. It proved to be efficient nanocatalyst for solvent-free synthesis of pyrano[3,2-c]pyridine derivatives under mild reaction conditions with good to excellent yields. This heterogeneous catalyst also exhibited higher activities than acid or base functionalized mesoporous silica, magnetic GO or basic Al_2O_3 an even higher than some basic homogeneous catalysts such as triethylamine and piperazine. More importantly, due to the loaded iron oxide nanoparticles, this catalyst could be easily recovered from the reaction mixture using an external magnet and reused without significant decrease in activity even after 7 runs.

How to cite this article
Rostamizadeh S, Hemmasi A, Zekri N. Magnetic amine-functionalized graphene oxide as a novel and recyclable bifunctional nanocatalyst for solvent-free synthesis of pyrano[3,2-c]pyridine derivatives. Nanochem Res, 2017; 2(1): 29-41. DOI: 10.22036/ncr.2017.01.004

INTRODUCTION

Pyrano[3,2-c]pyridine derivatives are important heterocyclic compounds with a vast range of biological, medicinal and pharmacological properties. They are constituents of antitumor, anti-flammatory, antifungal and antitubercular compounds [1-6]. In view of these useful properties, several methods have been reported for the synthesis of these interesting compounds. In the reported methods several catalysts such as sodium ethoxide [4], sodium [7], hexadecyltrimethylammonium bromide [8], KF-AL_2O_3 [9], sodium hydroxide, piperidine [10], organocatalyst [11], quinine [12], MCM-41-SO_3H [13], [BMIM]OH [14] and also different solvents such as BuOH [1,5,15], DMF [16,17], MeOH [7], H_2O [8], toluene [11,12], EtOH [18] have been used for the synthesis of pyrano[3,2-c]pyridines. These compounds also have been synthesized under catalyst-free [18] and solvent-free conditions [4,13]. Although these methods are quite satisfactory, they have one or more of drawbacks such as use of hazardous organic solvents, low yields of the products, extended reaction times and high temperatures.

Therefore, it is still desirable to seek a green and efficient protocol for preparation of these compounds. In recent years, most studies have been focused on homogeneous catalysts because of their high activity and selectivity [19,20]. The difficulty of recycling and reusing of these catalysts increases

* Corresponding Author Email: *shrostamizadeh@yahoo.com*

the cost and even pollution of the environment and/or final product [21,22]. An efficient method to overcome the problem of homogeneous catalysts is the heterogenization of active catalytic molecules and creating a heterogeneous catalytic system. However, the recovery of the heterogeneous catalysts from the final reaction mixture requires a filtration or centrifugation step and/or tedious work up. By using magnetic catalysts, they can be easily recovered by an external magnet. Among magnetic particles, Fe_3O_4 magnetic nanoparticles (MNPs) have received more attention due to their large specific surface area and good super paramagnetic property, which allows them to be separated simply by applying a magnetic field.

Recently, magnetic nanoparticles have been used as reusable catalysts in many organic transformations such as oxidation of alcohols [23,24], oxidation of cyclohexene [25], reduction of 4-nitrophenol [26,27] and synthesis of 4H-chromenes [28]. Magnetic nanocomposites have also some potential applications in different fields such as batteries, electrochemical display devices, magnetic evaporations, enzyme immunoassay, drug delivery [29-33] lipase immobilization [34] and synthesis of pyrano[3,2-c]chromenes, chromenes and spiro-oxindoles [35].

GO has attracted tremendous interest owing to its unique structural and surface properties [36,37]. The abundant oxygen containing surface functionalities, such as epoxide, hydroxyl and carboxylic acid groups make GO a potential starting material for immobilization of a large number of substances including a wide range of metals, biomolecules, fluorescent molecules, drugs, and inorganic nanoparticles [38-44]. Moreover, the presence of these functional groups makes GO sheets strongly hydrophilic, causing them to readily disperse in water [45-47]. Accordingly, these properties along with the large specific surface area have provided a desirable platform for loading magnetic nanoparticles onto GO [47-50]. In addition, GO could be an ideal carbocatalyst for using in a variety of chemical transformations, such as hydration, oxidation, C-H activation and polymerization [51]. However, GO has been used as a monofunctional catalyst based on its either high acidity or strong oxidization properties [52].

Due to the importance of Pyrano[3,2-c] pyridines and following of our interest towards the development of new catalysts for the synthesis of various organic compounds [13,18,52-61], herein we report the synthesis of a magnetic acid-base bifunctional catalyst by loading Fe_3O_4 nanoparticles onto the surface of GO sheets which have exhibited high activity for the synthesis of pyrano[3,2-c]pyridine derivatives through the reaction between malononitrile and 3,5-bis(benzylidene)-4-piperidone (Scheme 1).

EXPERIMENTAL

All chemicals were purchased from the Merck chemical company. Melting points were recorded on a Buchi B-540 apparatus. IR spectra were recorded on an ABB Bomem Model FTLA 200-100 instrument. ^{1}HNMR and ^{13}CNMR spectra were measured on a Bruker DRX-300 spectrometer at 300 and 75 MHz, using TMS as an internal standard and DMSO-d_6 as solvent. Chemical shifts (δ) were reported relative to TMS, and coupling constants (J) were reported in hertz (Hz). Mass spectra were recorded on a Shimadzu QP 1100 EX mass spectrometer with70 eV ionization potential. Elemental analyses for C, H and N were performed using a Heraeus CHN Rapid analyzer. X-ray powder diffraction (XRD) was carried out on a Philips X'Pert diffractometer with Cu Kα radiation. The structure and morphology of the products were characterized by transmission electron microscopy (TEM) and was recorded on a Philips CM-30 instrument on an accelerating voltage of 150 kV and scanning electron microscopy (SEM) analyses were performed by a Philips XL-30 instrument operating at an accelerating voltage of

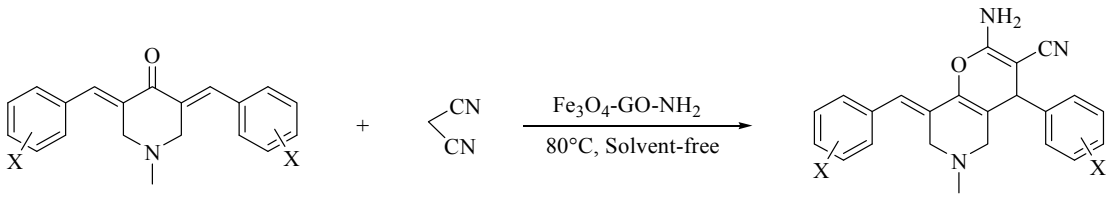

1 **2** **3 (a-n)**

Scheme 1. Fe_3O_4-GO-NH_2 as a magnetic nanocatalyst for the synthesis of pyrano[3,2-c]pyridine derivatives.

7.0 kV. The chemical compositions of the samples were evaluated by scanning electron microscopy (SEM, SAMX) equipped with an energy dispersive X-ray (EDX).

Preparation of Fe_3O_4-GO-NH_2

At first, Fe_3O_4-GO was prepared according to the previously reported method in the literature [62]. Then, a mixture of Fe_3O_4-GO (3g), 3-aminopropyltriethoxysilane (ATPES) (3.16 mL) in dry toluene (50 mL) was refluxed for 12 h. The catalyst was collected by an external magnet, washed with dichloromethane and diethyl ether and dried at 80°C for 2 h.

Preparation of 3,5-dibenzylidenepiperidin-4-ones

In a 50 mL reaction vial, a mixture of the 4-piperidone (10 mmol), an appropriate amount of aldehyde (20 mmol), 10% NaOH (1 mL) and 95% EtOH (30 mL) was stirred at room temperature for 0.5–2 h. The separated solid was collected by filtration and was recrystallized from ethanol for further purification [1].

General procedure for the synthesis of pyrano[3,2-c] pyridine derivatives in the presence of Fe_3O_4-GO-NH_2 under solvent-free conditions

A mixture of 3,5-dibenzylidenepiperidin-4-one (1mmol), malononitrile (2mmol) and Fe_3O_4-GO-NH_2 (30 mg) was ground thoroughly. It was then transferred into a reaction vessel and stirred at 80°C for an appropriate period of time. After completion of the reaction (monitored by TLC; petroleum ether and EtOAc, 2:1), the mixture was cooled down to room temperature and poured into the water (20 mL). The catalyst was then collected with an external magnet and the crude product was recrystallized from 95% EtOH to give the pure product.

Spectral data of some new and known synthesized compounds

(8E)-2-Amino-8-(2,3-dichlorobenzylidene)-4-(2,3-dichlorophenyl)-5,6,7,8-tetrahydro-6-methyl-4H-pyrano[3,2-c] pyridine-3-carbonitrile (Table 4, entry 1, compound 3a, $C_{23}H_{17}Cl_4N_3O$)

M.P: 215-217°C; IR (KBr) (ν cm^{-1}): 3332, 3260, 2202, 1678, 1637, 1601; ^{1}H NMR (300 MHz, DMSO-d_6), δ (ppm): 2.09 (3H, s, N-CH_3), 2.51 (1H, d, H-Pyridine, *J*=14.0 Hz), 3.02 (1H, d, H-Pyridine, *J*=16.2 Hz), 3.15 (1H, d, H-Pyridine, *J*=14.0 Hz), 3.31 (1H, d, H-Pyridine, *J*=14.8 Hz), 4.70 (1H, s, H-Pyran), 6.94 (1H, s, C=CH), 7.05 (2H, s, NH_2), 7.24-7.44 (4H, m, Ar-H), 7.58 (2H, d, Ar-H_4, *J*=8.0 Hz); ^{13}C NMR (75 MHz, DMSO-d_6), δ (ppm): 44.2, 53.7, 54.2, 118.8, 119.9, 128.0, 128.9, 129.2, 129.4, 129.6, 130.3, 130.6, 132.0, 136.3, 139.5, 142. 7, 160.1; MS (EI), *m/z* (%): 42 (100), 81 (47), 113 (30), 149 (70), 181 (61), 216 (54), 250 (91), 293 (12), 346 (11), 390 (14), 449 (19), 492 (22); Anal. Calcd for $C_{23}H_{17}Cl_4N_3O$: C, 56 %; H, 3.45 %; N, 8.52 %. Found: C, 56.03 %; H, 3.44 %; N, 8.55 %.

(8E)-2-Amino-8-(2-chlorobenzylidene)-4-(2-chlorophenyl)-5,6,7,8-tetrahydro-6-methyl-4H-pyrano[3,2-c] pyridine-3-carbonitrile (Table 4, entry 2, compound 3b, $C_{23}H_{19}Cl_2N_3O$)

M.p: 212-214 °C; ^{1}HNMR (300 MHz; DMSO-d_6), δ (ppm): 2.09 (3H, s, N-CH_3), 2.48-2.53 (1H, d, H-Pyridine, *J*= 14.6 Hz), 2.99 (1H, d, H-Pyridine, *J* = 16.1 Hz), 3.18 (1H, d, H-Pyridine, *J*= 14.0 Hz), 3.31 (1H, d, H-Pyridine, *J*= 17.0 Hz), 4.60 (1H, s, H-Pyran), 6.95 (1H, s, C=CH), 6.98 (2H, s, NH_2), 7.25-7.52 (8H, m, Ar-H); ^{13}CNMR(75 MHz, DMSO-d_6), δ (ppm): 44.3, 53.9, 54.3, 54.5, 56.0, 127.1, 128.1, 128.9, 129.0, 129.2, 129.4, 129.6, 130.5, 130.8, 131.0, 132.3, 132.8, 133.3, 133.9, 134.0, 139.4, 140.1,

159.5; MS (EI), *m/z* (%): 51 (36), 81 (62), 115 (66), 182 (100), 216 (89), 379 (53), 422 (74), 423 (45); Anal. Calcd for $C_{23}H_{19}Cl_2N_3O$: C, 65.1 %; H, 4.48 %; N, 9.90 %. Found: C, 65.07 %; H, 4.46 %; N, 9.91%.

(8E)-2-Amino-8-(4-chlorobenzylidene)-4-(4-chlorophenyl)-5,6,7,8-tetrahydro-6-methyl-4H-pyrano[3,2-c] pyridine-3-carbonitrile (Table 4, entry 4, compound 3d, $C_{23}H_{19}Cl_2N_3O$)

M.p: 239-242 °C; ^{1}HNMR (300 MHz; DMSO-d_6), δ (ppm): 2.16 (3H, s, N-CH_3), 2.98 (1H, d, H-Pyridine, *J*= 16.0 Hz), 3.20 (1H, d, H-Pyridine, *J*= 14.3 Hz), 3.28 (1H, d, H-Pyridine, *J*= 14.0 Hz), 3.46 (1H, d, H-Pyridine, *J*= 14.0 Hz), 4.16 (1H, s, H-Pyran), 6.87 (1H, s, C=CH), 6.88 (2H, s, NH_2), 7.25 (4H, d, Ar-$H_{1,5}$, *J*= 8.0 Hz), 7.43 (4H, d, Ar-$H_{2,4}$, *J*= 8.0 Hz); Anal. Calcd for $C_{23}H_{19}Cl_2N_3O$: C, 65.1 %; H, 4.48 %; N, 9.90 %. Found: C, 65.09 %; H, 4.49 %; N, 9.88%.

(8E)-2-Amino-8-(4-(benzyloxy)benzylidene)-4-(4-(benzyloxy)phenyl)-5,6,7,8-tetrahydro-6-methyl-4H-pyrano[3,2-c] pyridine-3-carbonitrile (Table 4, entry 12, compound 3l, $C_{37}H_{33}N_3O_3$)

M.p: 195-197 °C; ^{1}HNMR (300 MHz; DMSO-d_6), δ (ppm): 2.13 (3H, s, N-CH_3), 2.54 (1H, d, H-Pyridine, *J* = 14.4 Hz), 2.94 (1H, d, H-Pyridine, *J*= 14.0 Hz), 3.25 (1H, d, H-Pyridine, *J*= 14.4 Hz), 3.45 (1H, d, H-Pyridine, *J*= 14.0 Hz), 3.97 (1H, s,

H-Pyran), 5.06 (2H, s, OCH_2), 5.10 (2H, s, OCH_2), 6.75 (2H, s, NH_2), 6.83 (1H, s, C=CH), 7.00 (2H, d, Ar-H, *J*= 8.7 Hz), 7.03 (2H, d, Ar-H, *J*= 8.7 Hz), 7.12 (2H, d, Ar-H, *J*= 8.7 Hz), 7.18 (2H, d, Ar-H, *J*= 8.7 Hz), 7.29-7.46 (10 H, m, Ar-H): ^{13}CNMR (75 MHz, DMSO-d_6), δ (ppm): 44.4, 53.9, 54.4, 55.7, 113.0, 115.3, 115.5, 120.3, 120.4, 127.4, 129.4, 129.5, 130.9, 131.0, 132.3, 132.4, 139.1, 139.6, 139.7, 159.5, 159.6, 159.7, 162.8; MS (EI), *m/z* (%): 42 (16), 65 (63), 91 (100), 131 (40), 174 (44), 198 (19), 222 (23), 250 (63), 382 (86), 410 (54), 473 (30), 501 (75), 567 (16); Anal. Calcd for $C_{37}H_{33}N_3O_3$: C, 78.3 %; H, 5.82 %; N, 7.41 %. Found: C, 78.33 %; H, 5.80 %; N, 7.39 %.

(8E)-2-Amino-8-(naphthalen-1-yl-2-methylidene)-6-methyl-4-(naphthalen-1-yl)-5,6,7,8-tetrahydro-6-methyl-4H-pyrano[3,2-c]pyridine-3-carbonitrile (Table 4, entry 13, compound 3m, $C_{31}H_{25}N_3O$)

M.p.: 190-192 °C; IR (KBr) (ν cm^{-1}): 3329, 3182, 3052, 2933, 2189, 1684, 1638, 1497; ^{1}HNMR (300 MHz, DMSO-d_6), δ (ppm): 1.95 (3H, s, N-CH_3), 2.40 (1H, d, H-Pyridine, *J*= 15.7 Hz), 3.03 (1H, d, H-Pyridine, *J*= 15.8 Hz), 3.16 (1H, d, H-Pyridine, *J*= 13.7 Hz), 3.43 (1H, d, H-Pyridine, *J*= 14.0 Hz), 4.37 (1H, s, H-Pyran), 5.05 (1H, s, C=CH), 6.96 (2H, s, NH_2), 7.32 (1H, d, *J*= 6.5 Hz, Ar-H), 7.53 (7H, d, *J*= 8.3 Hz, Ar-H), 7.86 (2H, s, Ar-H), 7.96 (2H, d, Ar-H), 8.05 (1H, d, Ar-H), 8.37 (1H, s, Ar-H); ^{13}CNMR (75 MHz, DMSO-d_6), δ (ppm): 38.6, 38.9, 39.2, 39.5, 39.7, 40.0, 40.3, 44.3, 54.4, 54.7, 56.0, 56.3, 114.1, 119.0, 120.4, 123.1, 124.4, 125.4, 125.8, 126.2, 126.4, 126.8, 127.8, 128.5, 128.9, 131.3, 132.6, 133.2, 133.6, 139.5; MS (EI), *m/z* (%): 42(30.05), 128 (43.35), 141 (35.8), 152 (47.39), 165 (100), 232 (91.17), 283 (23.12), 388 (33.5), 411 (90.17), 455 (60.11); Anal. Calcd for $C_{31}H_{25}N_3O$: C, 81.76 %; H, 5.49 %; N, 9.23 %. Found: C, 81.78 %; H, 5.48 %; N, 9.20 %.

(8E)-2-Amino-8-(3-hydroxybenzylidene)-4-(3-hydroxyphenyl)-5,6,7,8-tetrahydro-6-methyl-4H-pyrano[3,2-c] pyridine-3-carbonitrile (Table 4, entry 14, compound 3n, $C_{23}H_{21}N_3O_3$)

M.P.: 245-247 °C; IR (KBr) (ν cm^{-1}): 3516, 2996, 2909, 2099, 1995, 1658, 1432; ^{1}H NMR (300 MHz, DMSO-d_6), δ (ppm): 2.14 (3H, s, CH_3), 2.59 (1H, s, H-Pyridine), 2.96 (1H, d, H-Pyridine, *J*= 15.9 Hz), 3.24 (1H, s, H-Pyridine), 3.45 (1H, d, H-Pyridine, *J*= 15.0 Hz), 3.9 (1H, s, H-Pyran), 6.61-6.64 (7H, m, C=CH, Ar-H), 6.80 (2H, s, NH_2), 7.14 (2H, m, Ar-H), 9.40 (1H, s, OH), 9.48 (1H, s, OH); ^{13}C NMR (75 MHZ, DMSO-d_6), δ (ppm): 39.50, 39.8, 40.0, 40.3, 41.0, 44.5, 54.3, 54.5, 55.9, 113.3, 114.2, 115.5, 118.3, 119.9, 121.5, 127.3, 129.5, 137.2, 139.0, 145.0, 157.3, 157.6, 159.7; MS (EI), *m/z* (%): 42 (46.11), 77 (41.1), 107 (82.2), 131 (60.5), 160 (36.1), 172 (30.5), 216 (35), 292 (41.1), 321(100), 387 (10); Anal. Calcd for $C_{23}H_{21}N_3O_3$: C, 71.32 %; H, 5.43 %; N, 10.85 %. Found: C, 71.30 %; H, 5.41 %; N, 10.86 %.

RESULT AND DISCUSSION

At the beginning, the prepared magnetic graphene oxide was reacted with 3-aminopropyltriethoxysilane (ATPES) to obtain the Fe_3O_4-GO-NH_2 (Scheme 2). This catalyst (Fe_3O_4-GO-NH_2) was characterized by IR, XRD, SEM, TEM, EDX techniques and acid-base

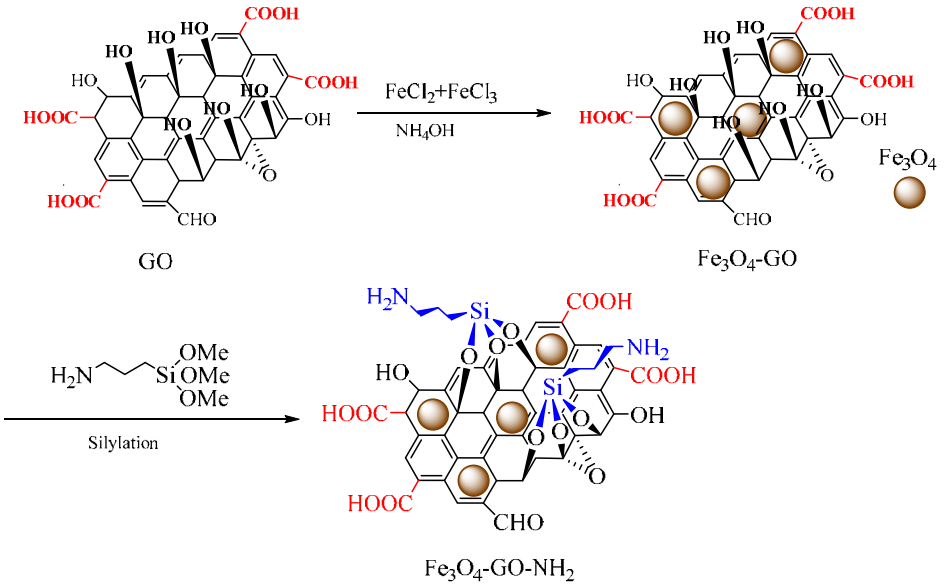

Scheme 2. Preparation of Fe_3O_4-GO-NH_2.

titration. Density of acidic groups in Fe_3O_4-GO-NH_2 determined by acid-base titration showed that the amount of H^+ in the catalyst is 2.5 mmol. g^{-1}.

FT–IR spectra of the catalyst

The functionalization of GO with magnetic Fe_3O_4 and –NH_2 was confirmed by Fourier-transform infrared (FT–IR). The FT-IR spectra of Go (a), Fe_3O_4-GO (b) and Fe_3O_4-GO-NH_2 (c) are shown in Fig. 1. The peak at 1738 cm^{-1} (Fig. 1.a) referred to the stretching band of C=O in carboxylic acid on the GO. The bands at 3364 and 1225 cm^{-1} were assigned to the stretching and bending of the O–H, respectively. The peak at 1624 cm^{-1} (aromatic C=C) could be attributed to the skeletal vibrations of unoxidized graphitic domains. The FT-IR spectrum of Fe_3O_4-GO samples differed from that of GO. The weakening of the peaks of C=O and O–H at 1738 and 3364 cm^{-1} respectively, are the evidences of this claim. The band around 587 cm^{-1} is indicative of Fe–O stretching vibrations, confirming the existence of Fe_3O_4.

In FT-IR spectra of Fe_3O_4-GO-NH_2, the bands in region of 3363-3404 cm^{-1} were attributed to the stretching vibration of (-NH_2) and two peaks at 2859 and 2924 cm^{-1}, indicative of symmetric and asymmetric stretching vibrations of C-H bands of CH_2-CH_2 groups connecting with the NH_2 group. Also, the band at 446 cm^{-1} was referred to the Fe-O stretching vibrations. Besides, the appearance of two peaks at 1041 and 1106 cm^{-1} was assigned to the O-Si-O asymmetric stretching and Si-O-C stretching vibration.

The XRD spectra of the catalyst

The X-ray powder diffraction (XRD) patterns of the synthesized nanocatalyst are presented in Fig. 2. The XRD analysis was performed from 1.0° (2θ) to 80.0° (2θ) in which the broad peaks at 1.0 (2θ) to 29 (2θ) are attributed to the amorphous state. Two peaks at 30° and 43° are due to the crystalline state of carbon of graphene and four peaks at 35°, 53.5°, 57°, and 62.5° are indexed to the crystalline state of cubic Fe_3O_4 nanoparticles. The XRD profile of Fe_3O_4-GO-NH_2 is consistent with the reported ones for the related compounds [62-64]. This confirms the structure of the synthesized catalyst (Fe_3O_4-GO-NH_2).

The SEM and TEM of the catalyst

The presence of Fe_3O_4 nanoparticles was confirmed by scanning electron microscopy (SEM) and transmission electron microscopy (TEM). The SEM showed that the bright dots of Fe_3O_4 nanoparticles were uniformly spread on the surface of GO. Also, in the TEM images, the black dots confirm the presence of Fe_3O_4 nanoparticles. The Fe_3O_4 nanoparticles with an average size of 13.6 nm are well decorated on the surfaces of the catalyst (Fig. 3).

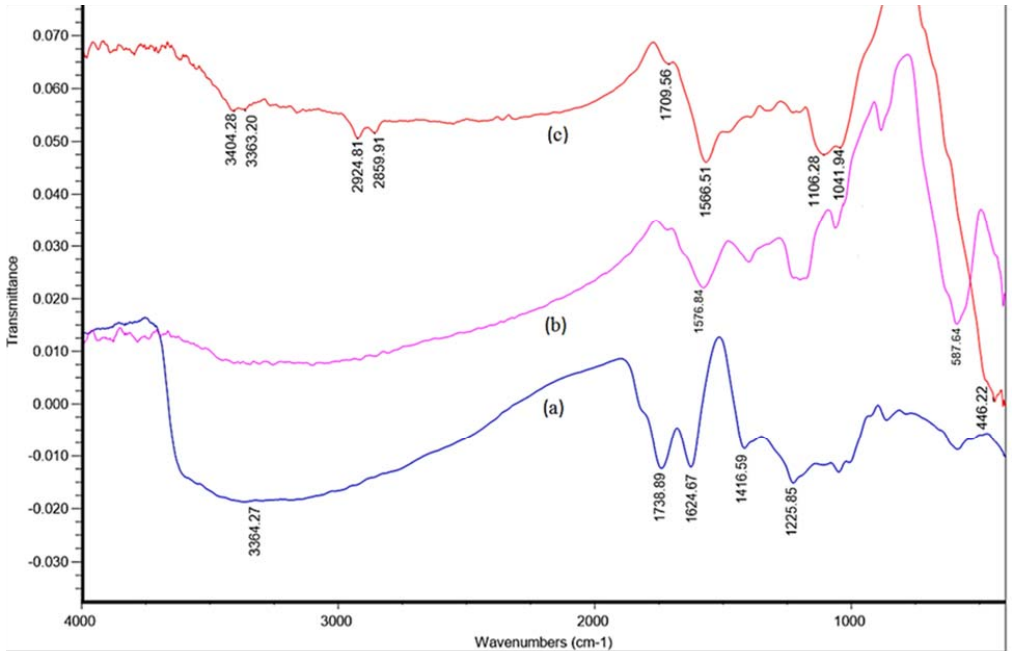

Fig. 1. FT-IR spectra of GO, Fe_3O_4-GO and Fe_3O_4-GO-NH_2.

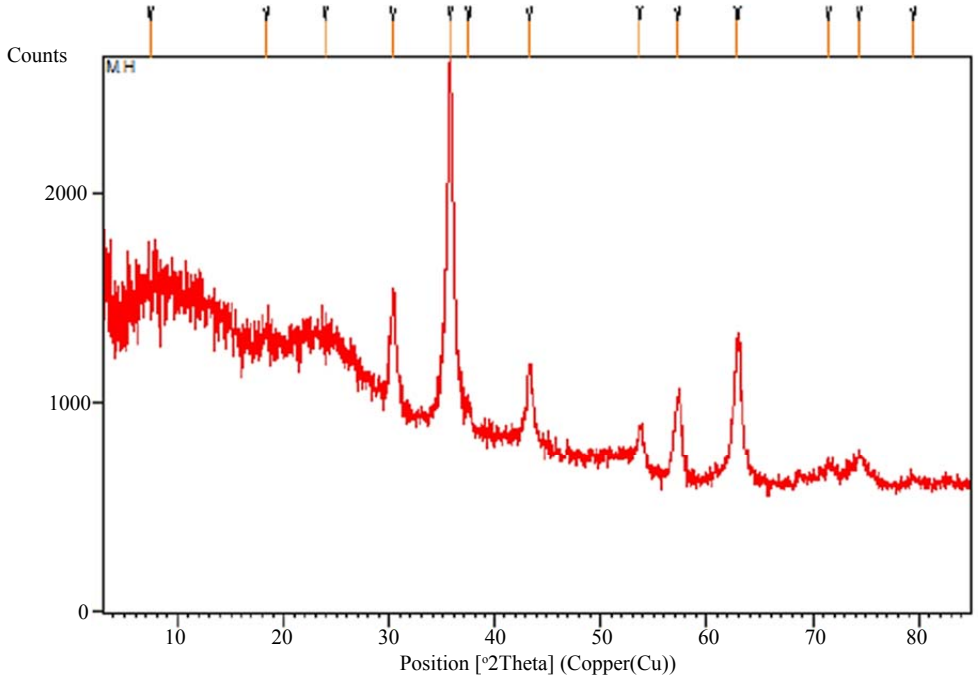

Fig. 2. The XRD pattern of Fe_3O_4-GO-NH_2.

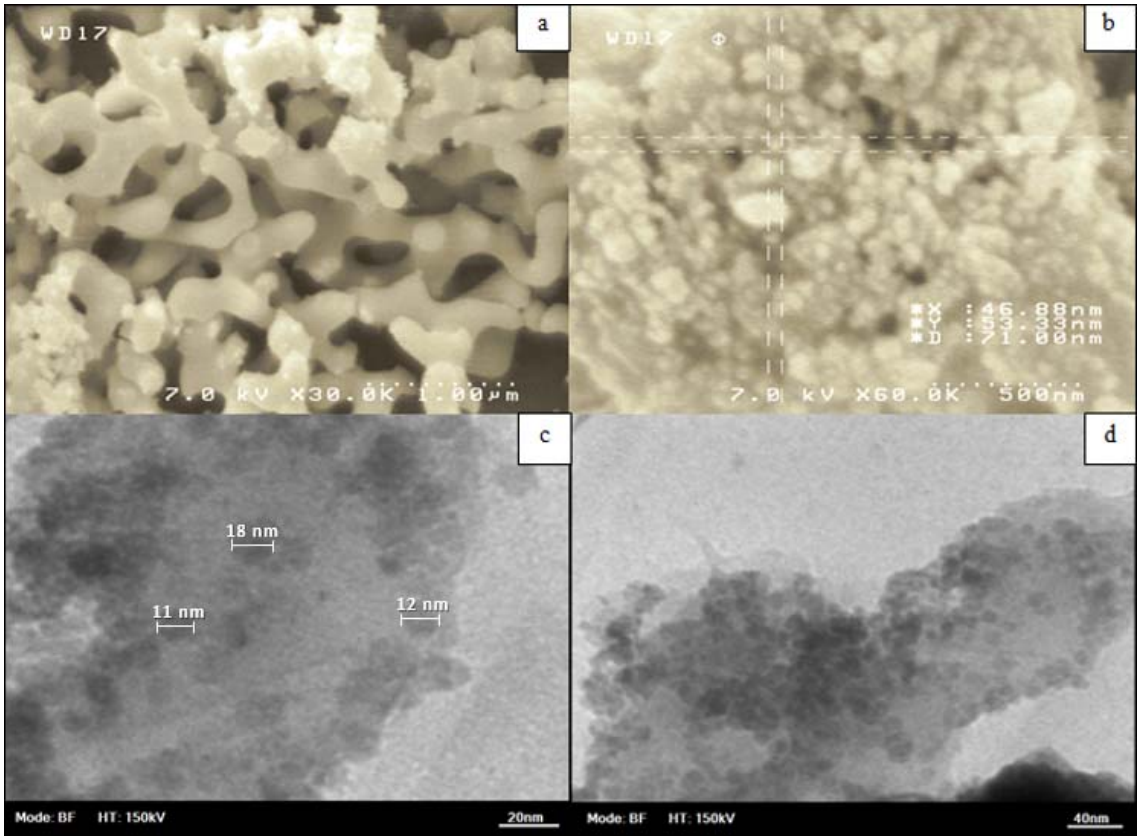

Fig. 3. (a and b) SEM images and (c and d) TEM images of the synthesized Fe_3O_4-GO-NH_2.

The EDX of the catalyst

The energy dispersive X-ray (EDX) spectrum of the catalyst was also recorded. All of the expected elements and embedded nanoparticles are observed according to relative peak surfaces (Fig. 4).

Synthesis of pyrano[3,2-c]pyridine derivatives catalyzed by Fe_3O_4-GO-NH_2 under solvent-free conditions

Fe_3O_4-GO-NH_2 was investigated in the synthesis of pyrano[3,2-c]pyridines. First, the reaction parameters such as malononitrile amount, catalyst amount ,solvent and temperature were optimized in the synthesis of (8E)-2-Amino-8-(4-chlorobenzylidene)-4-(4-chlorophenyl)-5,6,7,8-tetrahydro-6-methyl-4H-pyrano[3,2-c]pyridine-3-carbonitrile (3d) as a model reaction (Scheme 3).

In order to optimize the amount of malononitrile, different amounts of malononitrile were used (Table 1). As indicated in Table 1, when 2 mmol of the malononitrile was used for each mmol of 3,5-bis-(4-chlorobenzylidene)-1-methyl-piperidin-4-one, the best yield of 3d was obtained.

A comparison of the catalyst performance in the synthesis of 3d in various solvents is shown in Table 2. Among the solvents tested (MeOH, EtOH, PrOH, CH_3CN, H_2O, $CHCl_3$, H_2O/DMF) and solvent-free conditions, the best yield was obtained under solvent-free condition (Table 2). Finally, the reaction was performed at different temperatures under solvent-free conditions in which 80 °C was found to be the best.

In order to show the efficiency of Fe_3O_4-GO-NH_2 and compare its activity with other catalysts, the model reaction was performed in the presence

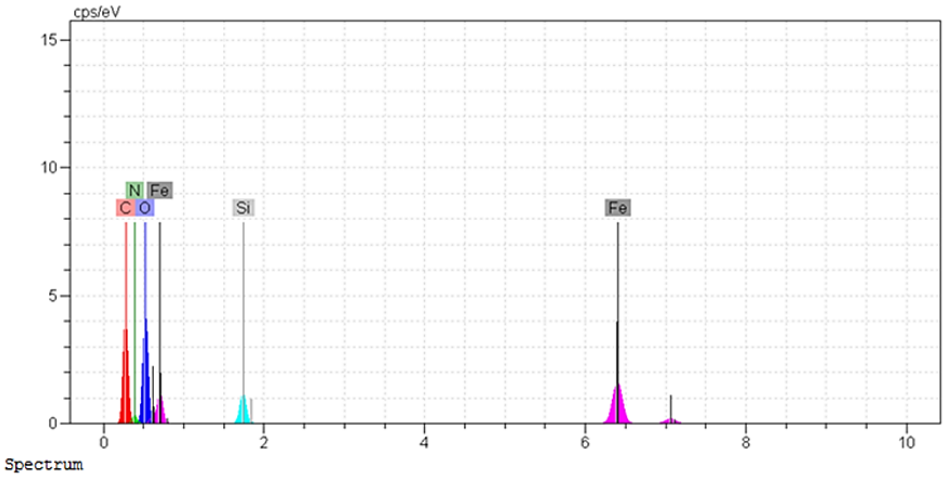

Fig. 4. The EDX spectra of Fe_3O_4-GO-NH_2.

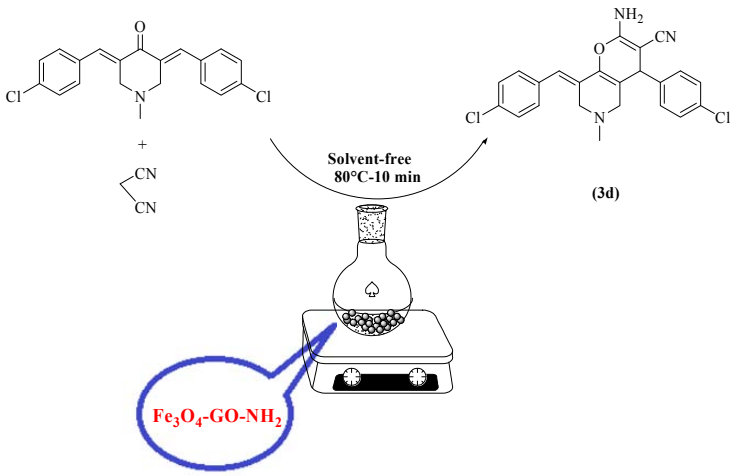

Scheme 3. Model reaction for the optimization.

of (α-Fe_2O_3)-MCM-41-SO_3H, (α-Fe_2O_3)-MCM-41-NH_2, KF/Al_2O_3, triethylamine, piperazine and GO-Fe_3O_4 (Table 3). The results show that the presence of amine groups in Fe_3O_4-GO-NH_2 catalyst (Table 3, entry 8), causes the reaction to complete faster as well as giving a higher yield of products than Fe_3O_4-GO (Table 3, entry 7). Although, the methods reported by our research group [13,18] show that running the reaction in the presence of (α-Fe_2O_3)-MCM-41-SO_3H under solvent-free conditions and also in the catalyst-free condition in EtOH, seem appealing at the first glance (Table 3, entry 1,2), yet such a procedure suffers from using higher temperature (115°C) along with lower yield of products for the first case [13] and also longer reaction times for the latter [18]. Hence, it is concluded that Fe_3O_4-GO-NH_2 is the most effective catalyst for the synthesis of pyrano[3,2-c]pyridine derivatives. The efficiency of this catalyst is due to the synergetic effects of –CO_2H as Brönsted acid, Fe^{3+} as Lewis acid and–NH_2 as base.

We then explored the synthesis of various pyrano[3,2-c]pyridine derivatives under optimized reaction conditions. In order to examine the scope and generality of the process, a variety of 3,5-bis-(benzylidene)-1-methyl-piperidin-4-ones possessing both electron-donating and electron-withdrawing groups were used. The results indicated that 3,5-bis-(benzylidene)-1-methyl-piperidin-4-ones with electron-withdrawing groups afforded shorter reaction times with higher yields (5a-5f, 5j, 5k). In contrast, those with electron-donating groups led to longer reaction times and lower yields (5h, 5i, 5l-5n).

A plausible mechanism is demonstrated in Scheme 4. Because of the two-dimensional structure

Table 1. Optimization of the amount of malononitrile[a].

Entry	Malononitrile (mmol)	Temperature (°C)	Yield (%)[b]
1	1	40	20
2	1.2	40	35
3	1.4	40	47
4	1.6	40	60
5	1.8	40	75
6	2	40	83

[a]3,5-bis-(4-chlorobenzylidene)-1-methyl-piperidin-4-one (1mmol), Fe_3O_4-GO-NH_2 (30 mg) were used in all experiments.
[b]Isolated yields.

Table 2. Optimization of the reaction conditions[a].

Entry	Solvent	T°C	Time/min	Yield (%)[b]
1	MeOH	64.7	35	87
2	EtOH	78.37	20	83
3	n-PrOH	97-98	45	65
4	CH_3CN	81.3	120	40
5	H_2O	100	300	No reaction
6	$CHCl_3$	61.2	300	No reaction
7	H_2O/DMF	120	40	80
8	Solvent-free	40	10	83
9	Solvent-free	60	10	90
10	Solvent-free	80	10	98
11	Solvent-free	100	10	97
12	Solvent-free	120	10	98

[a]3,5-bis-(4-chlorobenzylidene)-1-methyl-piperidin-4-one (1mmol), malononitrile (2mmol) and Fe_3O_4-GO-NH_2 (30 mg) were used in all experiments.
[b]Isolated yields.

Table 3. Comparison of the efficiency of different catalysts in the synthesis of 5d.

Entry	Catalyst[a]/ Solvent/ T (°C)	Time (min)	Yield (%)[b]
1	(α-Fe_2O_3)-MCM-41-SO_3H/ - / 115	10	93 [13]
2	Catalyst-free/ EtOH / rt	20	98 [18]
3	(α-Fe_2O_3)-MCM-41-NH_2 / - / 80	120	45
4	KF-Al_2O_3/ - / 80	600	Trace
5	Triethylamine/ - / 80	360	35
6	Piperazine/ - / 80	300	Trace
7	Fe_3O_4-GO/ - / 80	40	70
8	Fe_3O_4-GO-NH_2/ - /80	10	98

[a]The amount of all compared catalysts is 30 mg per 1mmol of reactants.
[b]Isolated yields.

Table 4. Synthesis of pyrano[3,2-c]pyridine derivatives in the presence of Fe_3O_4-GO-NH_2 as catalyst.

Entry		Product	Time (min)	Yield (%)[a]	M.P (ºC) Found	M.P (ºC) Reported
1	3a	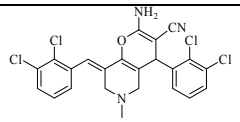	15	98	215-217	213-215 [18]
2	3b	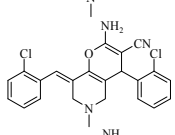	10	93	212-214	208-210 [4,11]
3	3c	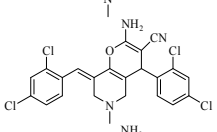	20	96	199-200	199-200 [4]
4	3d	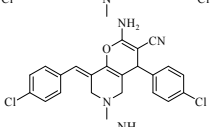	10	98	239-242	238-240 [18]
5	3e	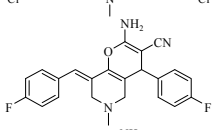	5	97	200-202	197-198 [11]
6	3f	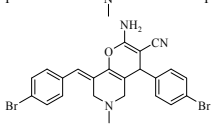	20	90	245-246	245-246 [18]
7	3g	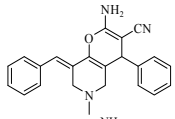	30	87	210-211	200-202 [18]
8	3h	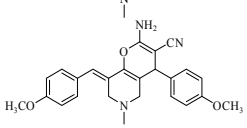	45	78	205-206	203-204 [1]
9	3i	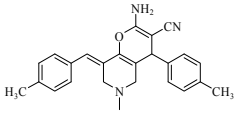	40	88	227-228	215-217 [17]
10	3j	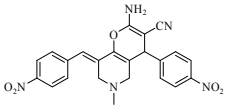	10	95	237-240	238-240 [17]
11	3k	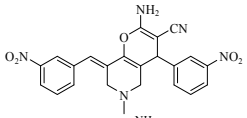	5	98	226-227	225-227 [17]
12	3l	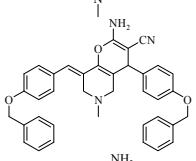	50	87	195-197	193-195 [18]
13	3m	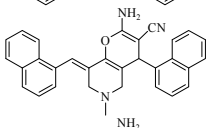	75	88	190-192	–
14	3n	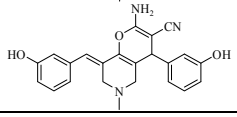	60	80	245-247	–

[a]Isolated yields.

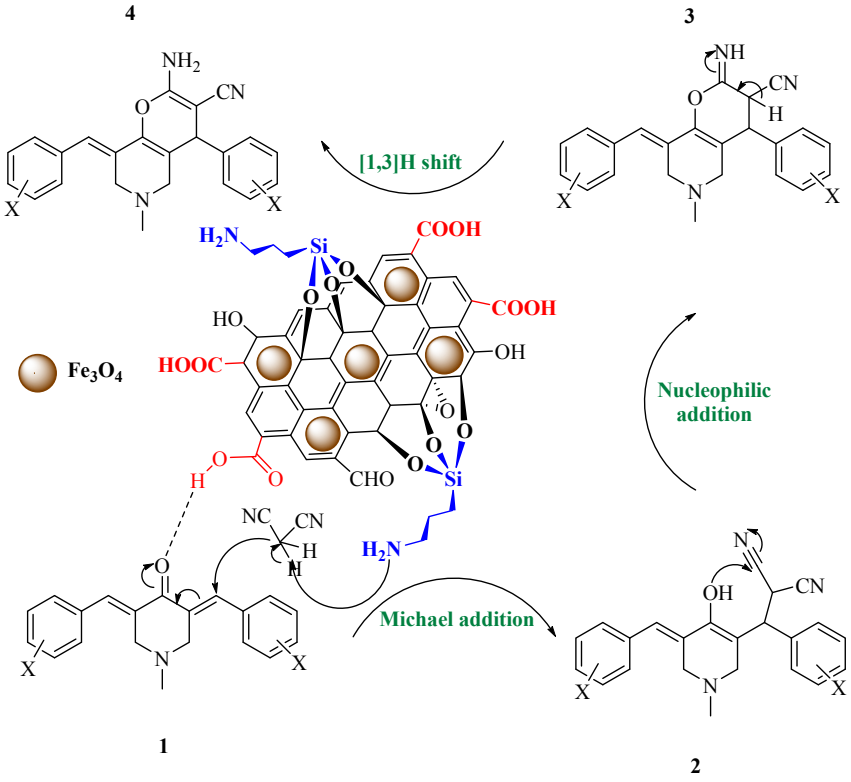

Scheme 4. A plausible mechanism for the synthesis of pyrano[3,2-c]pyridine in the presence of Fe_3O_4-GO-NH_2.

and the large specific surface area of Fe_3O_4-GO-NH_2, the reactants easily gain contact with the nanocatalyst. It should be mentioned that the process is facilitated by the assistance of Brönsted acidity of the intrinsic carboxylic acids on the edges of GO and Lewis acidity of Fe^{3+}, both of which are capable of bonding with the carbonyl oxygen of the 3,5-dibenzylidenepiperidin-4-one moiety. Afterwards, the amine groups at the surface of GO, remove the acidic hydrogen from malononitrile and make it facile for Michael addition to occurs between activated 3,5-dibenzylidenepiperidin-4-one (1) and malononitrile. Subsequently, intramolecular nucleophilic addition of hydroxyl (-OH) to one of the cyano groups in the intermediate (2), resulted in formation of the intermediate (3). Finally, through 1,3-H shift in the intermediate (3), the desired product is formed (4).

Reusability and stability of the catalyst

The recovery and reusability of the catalyst is an important benefit especially for commercial applications. Thus, the reusability of the prepared nanocatalyst was investigated in the model reaction under optimized reaction conditions. To do this, the Fe_3O_4-GO-NH_2 was collected by an external magnet. Then, the recovered catalyst was washed with ethyl acetate (3*10 mL), dried at 80°C and used in subsequent runs without observation of any significant decrease in activity even after 7 runs (Fig. 5). The ease of recovery of the reused catalyst by an external magnet, indicates that there is no considerable leaching of magnetic nanoparticles in the recovered catalyst even after seven times of reusing.

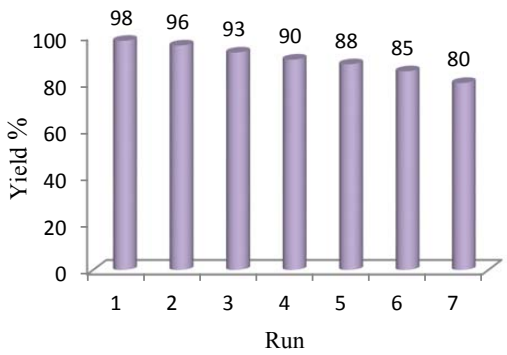

Fig. 5. Catalyst recovery at the end of the reaction in the model reaction.

CONCLUSION

In this research a new bifunctional magnetically recyclable nanocatalyst (Fe_3O_4-GO-NH_2) has been prepared and characterized by XRD, TEM, SEM, FT-IR, EDX and acid-base titration. It has shown a remarkable catalytic activity in the synthesis of pyrano[3,2-c]pyridine derivatives. This activity is due to combination of acidic functions (carboxylic acid groups on the edges of GO as Brönsted acid and Lewis acidity of the Fe^{3+}) to activate the oxygen moiety and basic function (the amine groups) to remove acidic hydrogen as well as large surface area of the catalyst. High yield of the desired product, short reaction time, ease of recovery and reusability of the catalyst, solvent-free and mild reaction condition are some advantages of the present work.

ACKNOWLEDGEMENTS

We gratefully acknowledge the support of this work from the K. N. Toosi University of Technology.

CONFLICT OF INTERESTS

The authors declare that there is no conflict of interests regarding the publication of this paper.

REFERENCES

1. El-Subbagh HI, Abu-Zaid SM, Mahran MA, Badria FA, Al-Obaid AM. Synthesis and Biological Evaluation of Certain α,β-Unsaturated Ketones and Their Corresponding Fused Pyridines as Antiviral and Cytotoxic Agents†. Journal of Medicinal Chemistry. 2000;43(15):2915-21.
2. Hammam AE-FG, Sharaf MA, Abd El-Hafez NA. ChemInform Abstract: Synthesis and Anticancer Activity of Pyridine and Thiazolopyrimidine Derivatives Using 1-Ethylpiperidone as a Synthon. ChemInform. 2001;32(26):no-no.
3. Gangjee A, Zeng Y, McGuire JJ, Kisliuk RL. Synthesis of Classical and Nonclassical, Partially Restricted, Linear, Tricyclic 5-Deaza Antifolates1. Journal of Medicinal Chemistry. 2002;45(23):5173-81.
4. Kumar RR, Perumal S, Senthilkumar P, Yogeeswari P, Sriram D. An atom efficient, solvent-free, green synthesis and antimycobacterial evaluation of 2-amino-6-methyl-4-aryl-8-[(E)-arylmethylidene]-5,6,7,8-tetrahydro-4H-pyrano[3,2-c] pyridine-3-carbonitriles. Bioorganic & Medicinal Chemistry Letters. 2007;17(23):6459-62.
5. Rostom SAF, Hassan GS, El-Subbagh HI. Synthesis and Biological Evaluation of Some Polymethoxylated Fused Pyridine Ring Systems as Antitumor Agents. Archiv der Pharmazie. 2009;342(10):584-90.
6. Ranjith Kumar R, Perumal S, Menéndez JC, Yogeeswari P, Sriram D. Antimycobacterial activity of novel 1,2,4-oxadiazole-pyranopyridine/chromene hybrids generated by chemoselective 1,3-dipolar cycloadditions of nitrile oxides. Bioorganic & Medicinal Chemistry. 2011;19(11):3444-50.
7. Girgis AS, Ismail NSM, Farag H. Facile synthesis, vasorelaxant properties and molecular modeling studies of 2-amino-8a-methoxy-4H-pyrano[3,2-c]pyridine-3-carbonitriles. European Journal of Medicinal Chemistry. 2011;46(6):2397-407.
8. Jin TS, Liu LB, Zhao Y, Li TS. Clean, One-Pot Synthesis of 4H-Pyran Derivatives Catalyzed by Hexadecyltrimethyl Ammonium Bromide in Aqueous Media. Synthetic Communications. 2005;35(14):1859-63.
9. Wang Xs, Shi Dq, Du Y, Zhou Y, Tu Sj. Synthesis of 2-Aminopyran Derivatives and 3-Arylpropionitrile Derivatives Catalyzed by KF/Al2O3. Synthetic Communications. 2004;34(8):1425-32.
10. Zhou J-F. One-Step Synthesis of Pyridine and 4H-Pyran Derivatives from Bisarylidenecyclohexanone and Malononitrile Under Microwave Irradiation. Synthetic Communications. 2003;33(1):99-103.
11. Hu Z-P, Lou C-L, Wang J-J, Chen C-X, Yan M. Organocatalytic Conjugate Addition of Malononitrile to Conformationally Restricted Dienones. The Journal of Organic Chemistry. 2011;76(10):3797-804.
12. Yan Z-PHJLX-GYX-JZM. Quinine-catalyzed enantioselective tandem conjugate addition/intramolecular cyclization of malononitrile and 1,4-dien-3-ones. Arkivoc. 2013;2013(3):1.
13. Rostamizadeh S, Shadjou N, Hasanzadeh M. Application of MCM-41-SO3H as an Advanced Nanocatalyst for the Solvent Free Synthesis of Pyrano[3,2-c]pyridine Derivatives. Journal of the Chinese Chemical Society. 2012;59(7):866-71.
14. Siddiqui IR, Srivastava A, Shamim S, Srivastava A, Waseem MA, Shireen, et al. Microwave accelerated facile and efficient synthesis of piperido[3′,4′:5,6]pyrano[2,3-d] pyrimidinones catalyzed by basic ionic liquid [BMIM]OH. Journal of Molecular Catalysis A: Chemical. 2014;382:126-35.
15. Al-Omar MA, Youssef KM, El-Sherbeny MA, Awadalla SAA, El-Subbagh HI. Synthesis andIn Vitro Antioxidant Activity of some New Fused Pyridine Analogs. Archiv der Pharmazie. 2005;338(4):175-80.
16. Tu S-J, Han Z-G, Jiang B, Yan S, Zhang X-H, Wu S-S, et al. An Efficient and Chemoselective Synthesis of 1,6-Naphthyridines and Pyrano[3,2-c]pyridines under Microwave Irradiation. Synthesis. 2009;2009(10):1639-46.
17. Wang S-L, Han Z-G, Tu S-J, Zhang X-H, Yan S, Hao W-J, et al. An efficient method for synthesis of pyrano[3,2-c] pyridine derivatives under microwave irradiation. Journal of Heterocyclic Chemistry. 2009;46(5):828-31.
18. Rostamizadeh S, Kassaee MZ, Shadjou N, Zandi H. Efficient synthesis of pyrano[3,2-c]pyridines via a green and catalyst-free method at ambient temperature, and related DFT calculations. Monatshefte für Chemie - Chemical Monthly. 2012;144(5):703-6.
19. Corma A, Garcia H. Silica-Bound Homogenous Catalysts as Recoverable and Reusable Catalysts in Organic Synthesis. Advanced Synthesis & Catalysis. 2006;348(12-13):1391-412.
20. Polshettiwar V, Luque R, Fihri A, Zhu H, Bouhrara M, Basset J-M. Magnetically Recoverable Nanocatalysts. Chemical Reviews. 2011;111(5):3036-75.
21. Wang D, Astruc D. Fast-Growing Field of Magnetically Recyclable Nanocatalysts. Chemical Reviews. 2014;114(14):6949-85.
22. M. B. Recoverable and Recyclable Catalysts. John Wiley & Sons, Ltd; 2009.

23. Sadri F, Ramazani A, Massoudi A, Khoobi M, Joo S. Magnetic CuFe2O4 nanoparticles as an efficient catalyst for the oxidation of alcohols to carbonyl compounds in the presence of oxone as an oxidant. Bulg Chem Commun. 2015;47(2):539-46.
24. Sadri F, Ramazani A, Massoudi A, Khoobi M, Tarasi R, Shafiee A, et al. Green oxidation of alcohols by using hydrogen peroxide in water in the presence of magnetic Fe3O4nanoparticles as recoverable catalyst. Green Chemistry Letters and Reviews. 2014;7(3):257-64.
25. Tarasi R, Ramazani A, Ghorbanloo M, Khoobi M, Aghahosseini H, Joo SW, et al. Preparation and Characterization of MCM-41@PEI·Mn as a New Organic-Inorganic Hybrid Nanomaterial and Study of its Catalytic Role in the Oxidation of Cyclohexene, Ethyl Benzene, and Toluene in the Presence of H2O2as an Oxidant. Bulletin of the Korean Chemical Society. 2016;37(4):529-37.
26. Veerakumar P, Velayudham M, Lu K-L, Rajagopal S. Silica-supported PEI capped nanopalladium as potential catalyst in Suzuki, Heck and Sonogashira coupling reactions. Applied Catalysis A: General. 2013;455:247-60.
27. Wang M-L, Jiang T-T, Lu Y, Liu H-J, Chen Y. Gold nanoparticles immobilized in hyperbranched polyethylenimine modified polyacrylonitrile fiber as highly efficient and recyclable heterogeneous catalysts for the reduction of 4-nitrophenol. Journal of Materials Chemistry A. 2013;1(19):5923.
28. Khoobi M, Ramazani A, Hojjati Z, Shakeri R, Khoshneviszadeh M, Ardestani SK, et al. Synthesis of Novel 4H-Chromenes Containing a Pyrimidine-2-Thione Function in the Presence of Fe3O4Magnetic Nanoparticles and Study of Their Antioxidant Activity. Phosphorus, Sulfur, and Silicon and the Related Elements. 2014;189(10):1586-95.
29. Shabanian M, Khoobi M, Hemati F, Khonakdar HA, ebrahimi SeS, Wagenknecht U, et al. New PLA/PEI-functionalized Fe3O4 nanocomposite: Preparation and characterization. Journal of Industrial and Engineering Chemistry. 2015;24:211-8.
30. Cruz-Montoya EDL, Rinaldi C. Influence of nanoparticle surface chemistry on the thermomechanical and magnetic properties of ferromagnetic nanocomposites. Journal of Polymer Science Part B: Polymer Physics. 2011;49(16):1163-72.
31. Gómez-Lopera SA, Arias JL, Gallardo V, Delgado ÁV. Colloidal Stability of Magnetite/Poly(lactic acid) Core/Shell Nanoparticles. Langmuir. 2006;22(6):2816-21.
32. Xu C, Ouyang C, Jia R, Li Y, Wang X. Magnetic and optical properties of poly(vinylidene difluoride)/ Fe3O4nanocomposite prepared by coprecipitation approach. Journal of Applied Polymer Science. 2009;111(4):1763-8.
33. Akrami M, Khoobi M, Khalilvand-Sedagheh M, Haririan I, Bahador A, Faramarzi MA, et al. Evaluation of multilayer coated magnetic nanoparticles as biocompatible curcumin delivery platforms for breast cancer treatment. RSC Adv. 2015;5(107):88096-107.
34. Khoobi M, Motevalizadeh SF, Asadgol Z, Forootanfar H, Shafiee A, Faramarzi MA. Synthesis of functionalized polyethylenimine-grafted mesoporous silica spheres and the effect of side arms on lipase immobilization and application. Biochemical Engineering Journal. 2014;88:131-41.
35. Khoobi M, Delshad TM, Vosooghi M, Alipour M, Hamadi H, Alipour E, et al. Polyethyleneimine-modified superparamagnetic Fe3O4 nanoparticles: An efficient, reusable and water tolerance nanocatalyst. Journal of Magnetism and Magnetic Materials. 2015;375:217-26.
36. Liu Y-W, Guan M-X, Feng L, Deng S-L, Bao J-F, Xie S-Y, et al. Facile and straightforward synthesis of superparamagnetic reduced graphene oxide–Fe3O4hybrid composite by a solvothermal reaction. Nanotechnology. 2012;24(2):025604.
37. Scheuermann GM, Rumi L, Steurer P, Bannwarth W, Mülhaupt R. Palladium Nanoparticles on Graphite Oxide and Its Functionalized Graphene Derivatives as Highly Active Catalysts for the Suzuki–Miyaura Coupling Reaction. Journal of the American Chemical Society. 2009;131(23):8262-70.
38. Goncalves G, Marques PAAP, Granadeiro CM, Nogueira HIS, Singh MK, Gracio J. Surface Modification of Graphene Nanosheets with Gold Nanoparticles: The Role of Oxygen Moieties at Graphene Surface on Gold Nucleation and Growth. Chemistry of Materials. 2009;21(20):4796-802.
39. Xu C, Wang X, Zhu J. Graphene–Metal Particle Nanocomposites. The Journal of Physical Chemistry C. 2008;112(50):19841-5.
40. Pasricha R, Gupta S, Srivastava AK. A Facile and Novel Synthesis of Agâ□□Graphene-Based Nanocomposites. Small. 2009;5(20):2253-9.
41. Cao A, Liu Z, Chu S, Wu M, Ye Z, Cai Z, et al. A Facile One-step Method to Produce Grapheneâ□□CdS Quantum Dot Nanocomposites as Promising Optoelectronic Materials. Advanced Materials. 2010;22(1):103-6.
42. Lu A-H, Salabas EL, Schüth F. Magnetic Nanoparticles: Synthesis, Protection, Functionalization, and Application. Angewandte Chemie International Edition. 2007;46(8):1222-44.
43. Frey NA, Peng S, Cheng K, Sun S. Magnetic nanoparticles: synthesis, functionalization, and applications in bioimaging and magnetic energy storage. Chemical Society Reviews. 2009;38(9):2532.
44. Stankovich S, Piner RD, Chen X, Wu N, Nguyen ST, Ruoff RS. Stable aqueous dispersions of graphitic nanoplatelets via the reduction of exfoliated graphite oxide in the presence of poly(sodium 4-styrenesulfonate). J Mater Chem. 2006;16(2):155-8.
45. Li D, Müller MB, Gilje S, Kaner RB, Wallace GG. Processable aqueous dispersions of graphene nanosheets. Nature Nanotechnology. 2008;3(2):101-5.
46. Park S, Ruoff RS. Chemical methods for the production of graphenes. Nature Nanotechnology. 2009;4(4):217-24.
47. Yang X, Zhang X, Ma Y, Huang Y, Wang Y, Chen Y. Superparamagnetic graphene oxide–Fe3O4 nanoparticles hybrid for controlled targeted drug carriers. Journal of Materials Chemistry. 2009;19(18):2710.
48. Shen J, Hu Y, Shi M, Li N, Ma H, Ye M. One Step Synthesis of Graphene Oxide–Magnetic Nanoparticle Composite. The Journal of Physical Chemistry C. 2010;114(3):1498-503.
49. Yang J, Tian C, Wang L, Fu H. An effective strategy for small-sized and highly-dispersed palladium nanoparticles supported on graphene with excellent performance for formic acid oxidation. Journal of Materials Chemistry. 2011;21(10):3384.
50. Chen X, Wu G, Chen J, Chen X, Xie Z, Wang X. Synthesis of "Clean" and Well-Dispersive Pd Nanoparticles with Excellent Electrocatalytic Property on Graphene Oxide. Journal of the American Chemical Society. 2011;133(11):3693-5.

51. Dreyer DR, Bielawski CW. Carbocatalysis: Heterogeneous carbons finding utility in synthetic chemistry. Chemical Science. 2011;2(7):1233.

52. Rostamizadeh S, Rezgi M, Shadjou N, Hasanzadeh M. Magnetic Graphene Oxide Anchored Sulfonic Acid as a Novel Nanocatalyst for the Synthesis of N-aryl-2-amino-1,6-naphthyridines. Journal of the Chinese Chemical Society. 2013;60(11):n/a-n/a.

53. Rostamizadeh S, Azad M, Shadjou N, Hasanzadeh M. (α-Fe2O3)-MCM-41-SO3H as a novel magnetic nanocatalyst for the synthesis of N-aryl-2-amino-1,6-naphthyridine derivatives. Catalysis Communications. 2012;25:83-91.

54. Rostamizadeh S, Nojavan M, Aryan R, Isapoor E. A Facile Synthesis of New Pyrazolo[3,4-d]pyrimidine Derivativesviaa One-Pot Four-Component Reaction with Sodium Acetate Supported on Basic Alumina as Promoter. Helvetica Chimica Acta. 2013;96(12):2267-75.

55. Rostamizadeh S, Estiri H, Azad M. Au anchored to (α-Fe2O3)-MCM-41-HS as a novel magnetic nanocatalyst for water-medium and solvent-free alkyne hydration. Catalysis Communications. 2014;57:29-35.

56. Rostamizadeh S, Nojavan M, Aryan R, Azad M. Dual Acidic Ionic Liquid Immobilized on α-Fe2O3–MCM-41 Magnetic Mesoporous Materials as the Hybrid Acidic Nanocatalyst for the Synthesis of Pyrimido[4,5-d]pyrimidine Derivatives. Catalysis Letters. 2014;144(10):1772-83.

57. Rostamizadeh S, Nojavan M, Aryan R, Isapoor E, Azad M. Amino acid-based ionic liquid immobilized on α-Fe2O3-MCM-41: An efficient magnetic nanocatalyst and recyclable reaction media for the synthesis of quinazolin-4(3H)-one derivatives. Journal of Molecular Catalysis A: Chemical. 2013;374-375:102-10.

58. Rostamizadeh S, Zekri N, Tahershamsi L. Nanosilica Supported Dual Acidic Ionic Liquid as a Recyclable Catalyst for the Rapid and Green Synthesis of Polycyclic Phenolic Compounds. Polycyclic Aromatic Compounds. 2014;34(5):542-60.

59. Rostamizadeh S, Zekri N. Synthesis of substituted trisphenols by use of a double acidic ionic liquid under solvent-free conditions. Iranian Journal of Catalysis. 2014;4(4):253-60.

60. Rostamizadeh S, Zekri N, Tahershamsi L. Nanosilica-supported dual acidic ionic liquid as a heterogeneous and reusable catalyst for the synthesis of flavanones under solvent-free conditions. Chemistry of Heterocyclic Compounds. 2015;51(6):526-30.

61. Rostamizadeh S, Tahershamsi L, Zekri N. An efficient, one-pot synthesis of pyrido[2,3-d:6,5-d′]dipyrimidines using SBA-15-supported sulfonic acid nanocatalyst under solvent-free conditions. Journal of the Iranian Chemical Society. 2015;12(8):1381-9.

62. Kassaee MZ, Motamedi E, Majdi M. Magnetic Fe3O4-graphene oxide/polystyrene: Fabrication and characterization of a promising nanocomposite. Chemical Engineering Journal. 2011;172(1):540-9.

63. Mondal J, Nguyen KT, Jana A, Kurniawan K, Borah P, Zhao Y, et al. Efficient alkene hydrogenation over a magnetically recoverable and recyclable Fe3O4@GO nanocatalyst using hydrazine hydrate as the hydrogen source. Chem Commun. 2014;50(81):12095-7.

64. Metin Ö, Aydoğan Ş, Meral K. A new route for the synthesis of graphene oxide–Fe3O4 (GO–Fe3O4) nanocomposites and their Schottky diode applications. Journal of Alloys and Compounds. 2014;585:681-8.